

## Synthesis of Molecularly Imprinted Polymer for the Selective Removal of Mercury

Faraz Ahmed Mustafai<sup>1</sup>, Aamna Balouch<sup>1\*</sup>, Muhammad Iqbal Bhangar<sup>2</sup>, Abdullah<sup>1</sup>, Kausar Rajar<sup>1</sup>, Pirah Panah<sup>1</sup>, Bilal Ahmed<sup>3</sup>, Tariq Shah<sup>1</sup>, Ameet Kumar<sup>1</sup>

<sup>1</sup> National Centre of Excellence in Analytical Chemistry, University of Sindh, Jamshoro, PAKISTAN

<sup>2</sup> International Centre for Chemical and Biological Science, University of Karachi, Karachi, PAKISTAN

<sup>3</sup> Institute of Physics, University of Sindh, Jamshoro, PAKISTAN

Received 19 April 2018 • Revised 4 June 2018 • Accepted 17 July 2018

### ABSTRACT

An adsorbent consisting of Hg<sup>2+</sup> ion imprinted polymer (IIP) was prepared and used for removal of Hg<sup>2+</sup> from real water samples. IIP was synthesized by utilizing 1-vinylimidazole and methacrylic acid as complexing agent and monomer. IIP was characterized by FT-IR, SEM and EDX to investigate the functionality, morphology and elemental analysis. Adsorption isotherms and kinetics of Hg<sup>2+</sup> ion on Hg<sup>2+</sup> imprinted polymer have been studied and adsorption phenomenon of IIP was found to follow the Langmuir isotherm and pseudo second order kinetic model. Other parameters such as pH, temperature, shaking speed, and agitation time affecting the adsorption of Hg<sup>2+</sup> were also optimized. The relative selectivity coefficient of imprinted polymer for Hg<sup>2+</sup> / Cu<sup>2+</sup>, Hg<sup>2+</sup> / Cr<sup>3+</sup>, Hg<sup>2+</sup> / Co<sup>2+</sup> were 122, 103, 76, respectively.

**Keywords:** imprinted polymer, Hg<sup>2+</sup>, selective recognition, adsorption, toxicity, drinking water

### INTRODUCTION

Mercury is a toxic element which exists in the natural environment; it is a constituent of earth's crust and is present in aquatic sediments, soil, water, air, animals and living plants [1]. Nearly 3400 metric tons of elemental mercury is released into global environment per year and approximately 95% remains in terrestrial soil, 3% in surface ocean water, and 2% in the atmosphere. Around 70% of the mercury pollutant comes in the environment through anthropogenic sources [24]. Mercury is a harmful pollutant in the biosphere and considered to be a human health hazard. When it enters the body, it binds with sulfhydryl groups to inactivate key enzymes responsible for preventing oxidative damage and causes symptoms of neurological damage, kidney and liver toxicity [2,3,4,5].

Production of mercury-containing products is progressively increasing; it is essential in manufacturing of thermometers, batteries, cathode tubes, cameras, medical laboratory chemicals and equipment, and has been used as a catalyst in the production of urethane polymers for plastics, a cathode in the production of chlorine mercury vapor lamps and barometers. Hence, monitoring mercury level in environment is very much essential [6].

To clear the aqueous environment of mercury contamination, many pre-concentration and separation methods are stated; photo-catalysis [7], biological processing [8], Solid Phase Extraction (SPE), Cloud Point Extraction (CPE), solid and liquid phase micro extraction [9] ion exchange precipitation, co-precipitation, chemical precipitation [10] complexation, flotation [11], coagulation, electrodeposition and membrane filtration [12], electrochemical [13] bio-filtration [14] electrolysis and cementation [15].

Hence, selectivity is a requiring consequence and it is hard to accomplish with methods and materials defined earlier. To deal with the alarming problem and to get better selectivity, Molecular Imprinted Polymer (MIP) has

© 2018 by the authors; licensee Modestum Ltd., UK. This article is an open access article distributed under the terms and conditions of the Creative Commons Attribution License (<http://creativecommons.org/licenses/by/4.0/>).

✉ faraz\_ahmed1992@hotmail.com ✉ aamna\_balouch@yahoo.com (\*Correspondence)

✉ dbhangar2000@yahoo.com ✉ anachemist31@gmail.com ✉ kosarraj12@gmail.com

✉ pirah.panah@gmail.com ✉ bilal\_ahmed8562@yahoo.com ✉ tariq\_shah2009@yahoo.com

✉ ameeek03@gmail.com

been synthesized. MIP's have recognition characteristics [16] with non-covalent approach. In MIP's, a template molecule interacts with a functional monomer and a crosslinker in a porogen solvent [17] and after successful polymerization, the removal of the template generates the recognition cavities inside the three-dimensional copolymer network. Nishidi in 1976 introduced Ion Imprinted Polymers (IIP's) similar to MIP's differ only by template molecule which is metal ion in IIP's [18].

In this study, Hg<sup>2+</sup> ion imprinted polymer (IIP) is synthesized by precipitation copolymerization by utilizing methacrylic acid (MAA) as a monomer, 1-vinylimidazole as a specific ligand for Hg<sup>2+</sup> ions and ethylene glycol dimethacrylate (EGDMA) as a cross-linker. Fourier Transform Infrared Spectroscopy (FT-IR), Scanning Electron Microscopy (SEM), and Electron Diffraction X-ray (EDX) were used for the characterization. Factors affecting the separation were studied and optimized pH of solutions, desorption, and sorption rate.

## EXPERIMENTAL SETUP

### Materials

Methacrylic acid (MAA), ethyleneglycoldimethacrylate (EGDMA), 2,2'-azobisisobutyronitrile (AIBN), 1-vinylimidazole were obtained from Aldrich (USA), Mercuric chloride (HgCl<sub>2</sub>), and methanol and other chemicals were obtained from Merck, Germany.

### Instrumentation

A Flame Atomic Absorption Spectrophotometer (FAAS) (Perkin-Elmer Model Analyst 700, Norwalk, CT) was used for the determination of selected metals. To acquire maximum absorbance signal, adjustments in the acetylene flow rate and the burner height were made. pH meter, a Metrohm 781 pH meter was used for pH adjustments. Milli-Q machine and ultrapure (Milli-Q) water were obtained from Milli-Q water purification machine (Elga Co. USA.) Ultrasonicator, electronic balances, magnetic Stirrer and heating instruments were used during all experiments work.

### Synthesis of Hg<sup>2+</sup> Imprinted Polymer

Hg<sup>2+</sup> ion imprinted polymer was prepared via thermal precipitation polymerization technique. 1.5mmol of HgCl<sub>2</sub>, and 6.0mmol of 1-vinylimidazole 6.0mmol of MAA were dissolved in 10mL of methanol and sonicated for 30 minute for complexation, then 30mmol of EGDMA and 0.009g of AIBN were dissolved 10mL of methanol and added in a 50mL reaction flask. Polymerization was performed at 60°C with for next 18 hours under nitrogen environment. Non-imprinted polymer was also prepared through same procedure without template (Hg<sup>2+</sup> ions). Afterwards IIP and NIP were washed with MeOH:H<sub>2</sub>O repeatedly to remove un-reacted materials.

### Leaching of the Hg<sup>2+</sup> Ions from Imprinted Polymer

Hg<sup>2+</sup> ion imprinted polymer stirred for 30 minutes in 1M HCl, and the method was repeated 5 times to accomplish leaching of Hg<sup>2+</sup> ions, than, washed with D.I water until neutral pH was achieved. Then, the polymer was dried in vacuum oven at 70°C.

## RESULTS AND DISCUSSION

### Characterization of the Hg<sup>2+</sup>-Imprinted Polymer

#### Scanning Electron Microscopy (SEM)

Surface and morphology investigation of the synthesized IIP's were done by using back-scatter detector. **Figure 3** shows the difference between the SEM images of IIP's. NIP (A) has uniform and smooth surface, while at another hand SEM image of IIP (B) exhibits a fractured and irregular surface due to the imprinting of Hg<sup>2+</sup> ions in polymeric material, and in contrast to NIP and IIP, the polymer after leaching of Hg<sup>2+</sup> ions(C) possesses porosity in the polymeric material which facilitates the binding of the template ions.

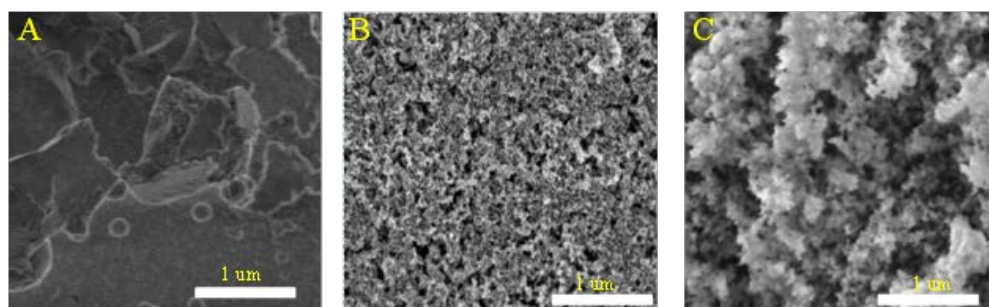


**Figure 1.** SEM images for (A) NIP (B) IIP(C) IIP after the leaching o

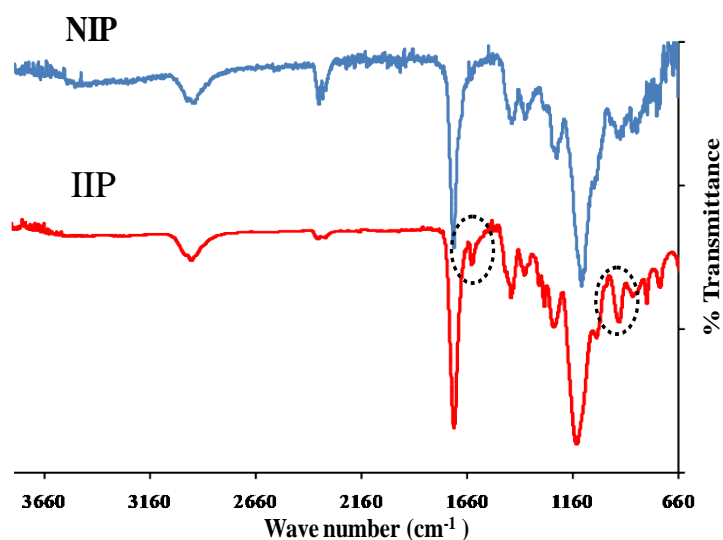


**Figure 2.** FT-IR (blue line) NIP and (red line) I

### *Fourier Transform Infrared spectroscopy*

In order to ascertain the imprinting of  $\text{Hg}^{2+}$  ions in polymer matrix, the FT-IR analysis were carried out by using KBr pellet method. **Figure 2** shows the FT-IR spectra of both NIP and Hg-IP, the similarity between these IR spectra means that both the polymers have same backbone [25]. The peak at  $911\text{ cm}^{-1}$  in fingerprint region is characteristic for the  $\text{Hg}^{2+}$  ion and, other peak observed at  $1600\text{ cm}^{-1}$  in (**Figure 2A**) Hg-IIP due to  $-\text{C}=\text{C}$  and  $\text{C}=\text{N}$  which is reduced in (**Figure 2B**) NIP spectra. This amount of reduction in band frequency is evidence for the coordination of the  $\text{Hg}^{2+}$  ions with non-bonding electron pairs of nitrogen in N-C group in 1-vinylimidazole. The peak at  $1710\text{ cm}^{-1}$  is responsible for ester carbonyl group. The bands at  $1160\text{ cm}^{-1}$ ,  $1200\text{ cm}^{-1}$  were assigned to the asymmetric and symmetric modes of C-O-C bonds and C-C bonds in ester group, whereas, bands at  $2960\text{ cm}^{-1}$  and  $2926\text{ cm}^{-1}$  are accounts for the stretching vibration mode of the aliphatic C-H groups [19].

### *Energy-dispersive X-ray spectroscopy (EDX)*

To confirm the formation of NIP, IIP, and presence and absence of  $\text{Hg}^{2+}$  ions after leaching from IIP, the elemental analysis was conducted by Energy-dispersive X-ray spectroscopy (EDX). **Figure 3A** NIP with three major peaks corresponds to O, C, and S and, there is no other signal which confirms the purity of polymer. The IIP shown in **Figure 3B** has an extra peak of  $\text{Hg}^{2+}$  ion in the spectrum which is the evidence for the successful imprinting of the  $\text{Hg}^{2+}$  ions. Absence of  $\text{Hg}^{2+}$  ions signal in **Figure 3C** EDX spectra of IIP after removal of template confirms the leaching of  $\text{Hg}^{2+}$  ions from polymeric material.

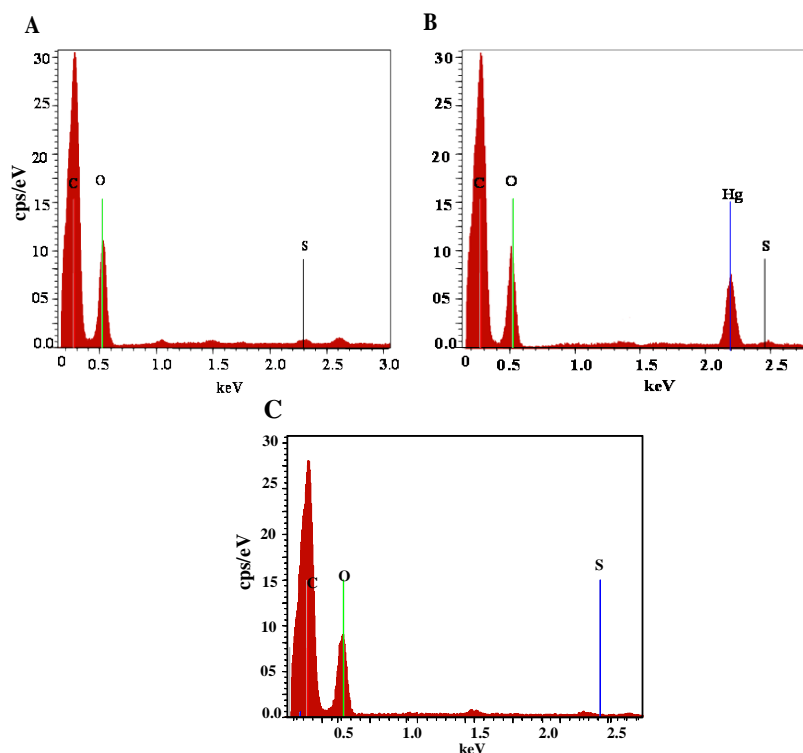


**Figure 3.** EDX spectra for (A) NIP (B) IIP (C) IIP after the leaching of  $\text{Hg}^{2+}$  ions

### Adsorption of $\text{Hg}^{2+}$ Ions on IIP

The containing power of IIP to adsorb  $\text{Hg}^{2+}$  ions were studied via batch experiment by equilibrating 20 mg of adsorbent in 20 mL of  $1.0 \text{ mgL}^{-1}$  mercury standard, stirred at 200rpm for 30minutes. Then, the solution was filtered and filtrate was analyzed by AAS via cold vapor method to check the unadsorbed concentration of  $\text{Hg}^{2+}$  ions. Initial and final concentration of samples was analyzed against mercury standard and results were obtained. Later on real samples were also collected from diverse drinking water sources and were analyzed before and after the adsorption.

### Point of zero charge ( $\text{pH}_{\text{PZC}}$ )

Point of zero charge tells the pH at which the net electric charge of cation and anion become zero on the adsorbent surface. The initial pH of solutions was adjusted by adding either NaOH or HCl in the range of 2-10. Then 20 mg of adsorbent were added in series of 50 mL conical flask containing 20 mL of pH adjusted solution and shaken for next 24 hours at ambient temperature at 200 rpm [20]. Afterwards, final pH values were noted and, the initial and final pH ( $\text{pH}_i$  and  $\text{pH}_f$ ) values ( $\text{pH} = \text{pH}_i - \text{pH}_f$ ) were plotted against the  $\text{pH}_i$ . The point of intersection of the resulting curve  $\text{pH}_{\text{PZC}}$  value. The value of  $\text{pH}_{\text{PZC}}$  was found to be 5.1, which is shown in [Figure 4](#). Above  $\text{pH}_{\text{PZC}}$  value adsorbent has negative charge. This result is in agreement with the obtained pH results at which optimum adsorption achieved.

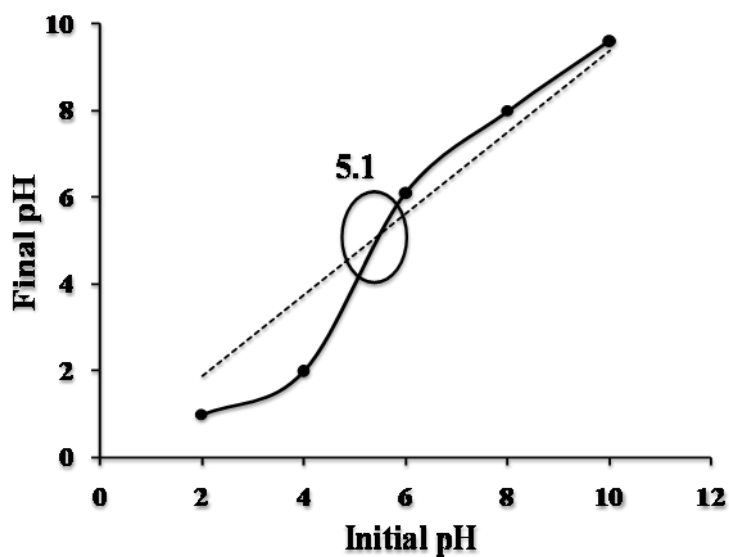


Figure 4. Plot of  $pH_i$  vs.  $\Delta pH$  to obtain point of zero charge ( $pH_{pzc}$ ) value for the IIP

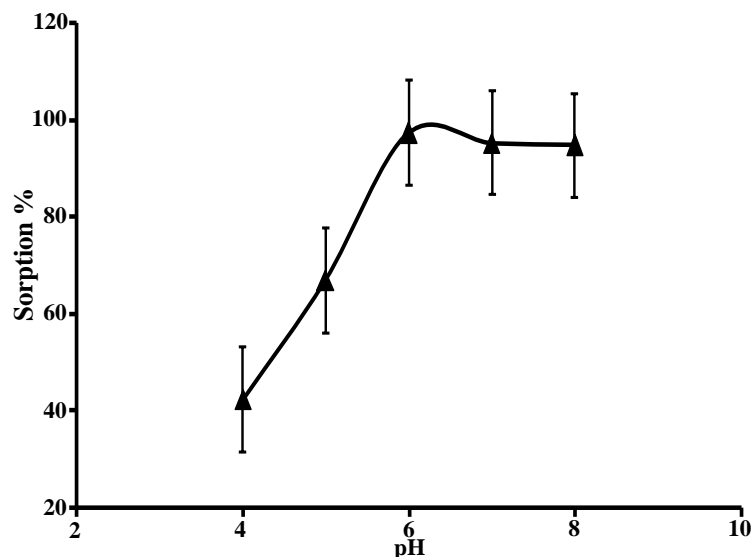


Figure 5. Effect of pH on adsorption of  $Hg^{2+}$  ions

### Effect of pH

Adsorption of metal ion is firmly pH dependent, thus effect of pH studied by equilibrating 20 mg of polymer as adsorbent with 20 mL of aqueous solution containing  $1.0 \mu g L^{-1}$  concentration of  $Hg^{2+}$  ions in adjusted pH range of 4-8. Figure 5 shows the increased in extraction with the increased pH and maximum adsorption achieved at pH 6. Low extraction at decreased pH could be because of the hindrance of the  $H^+$  ion and as the mere pH increased protonation weekend and uptake of  $Hg^{2+}$  ions favored. Adsorption diminishes as the pH increases formation of  $OH^-$  ion increases. Therefore, pH of solution adjusted to pH 6 for the optimum extraction of  $Hg^{2+}$  ions [21].

### Effect of contact time

The effect of sorption and desorption time on the adsorption of  $Hg^{2+}$  ions was also studied through a batch experiment as contact time plays vital role in the adsorption phenomenon. The adsorption of  $Hg^{2+}$  ions was investigated at 30 to 240 minutes at pH 6 and the results are presented in Figure 6. Initially the increase in adsorption was observed when reaction was proceeding from 30 to 60 and 90 minutes respectively. Maximum adsorption was accomplished in 90 minutes. After the 90 minute reaction time the adsorption was declined which

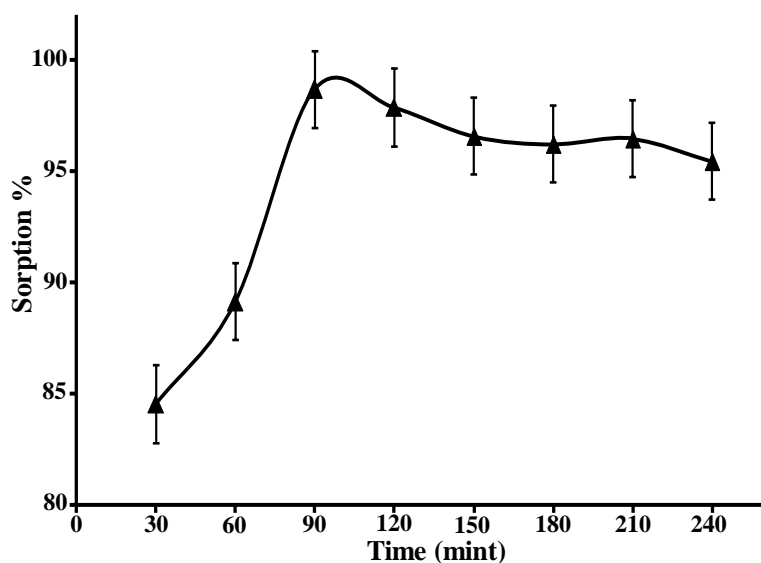


**Figure 6.** Effect of contact time on the adsorption of  $Hg^{2+}$  ions

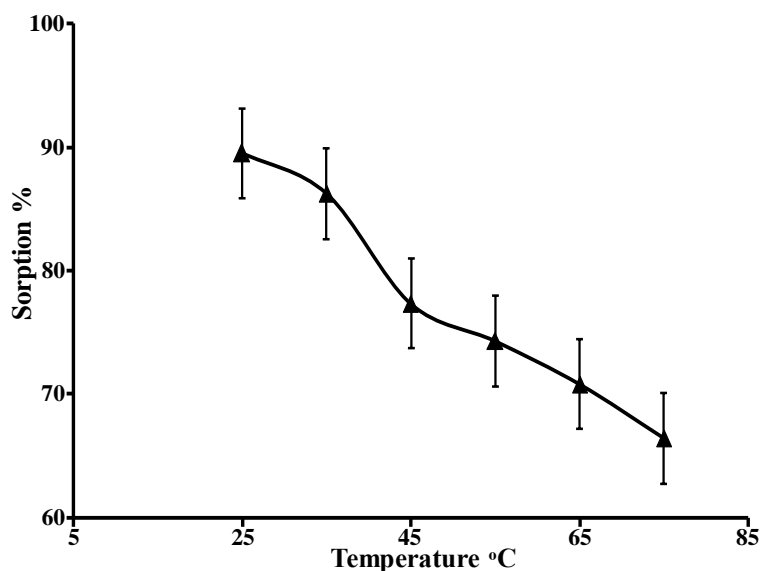


**Figure 7.** Effect of temperature on the adsorption of  $Hg^{2+}$  ions

could be due to disturbance of equilibrium established between sorbate and sorbent. Further reaction was conducted up to 240 minutes and checked the adsorption efficiency, and it was cleared from the data that with increase in time decrease in adsorption was observed. Therefore the 90 minute reaction time was taken as the optimum contact time for further studies [22].

### *Effect of temperature*

Adsorption mechanism has great dependence on the temperature as the mobility of ions is greatly affected by the temperature and ions collide and attach with adsorbent when they easily move in solution. To investigate the temperature affect, adsorption studies were carried out at different temperatures from 25°C to 75°C at optimized pH and time and results are presented in [Figure 7](#). At 25°C maximum adsorption of  $Hg^{2+}$  ions occurred and as the temperature increased a decline in adsorption of  $Hg^{2+}$  ions is observed from above it can be said that at high temperature adsorption is shifting toward desorption. So, 25°C were taken as the optimized temperature [23].

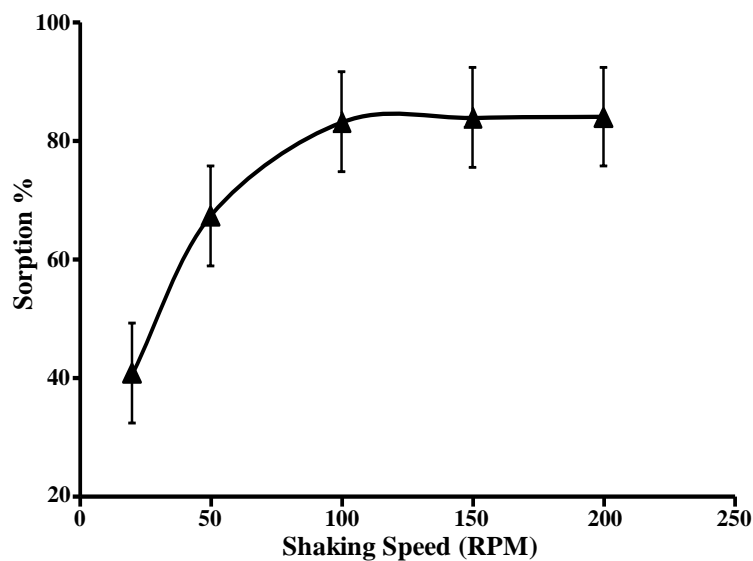


**Figure 8.** Effect of shaking speed on adsorption  $\text{Hg}^{2+}$  ions

### *Effect of shaking speed*

Effect of shaking speed over the uptake of  $\text{Hg}^{2+}$  ions was also studied at different shaking speed from 20 to 200rpm via batch experiment with other optimum parameters. Initially rise in the adsorption was observed from 20 to 100rpm and optimum adsorption achieved at 100rpm, shown in **Figure 8**, while a little decline is noticed at increased shaking speed and it can be said at above shaking speed desorption occurred.

### *Adsorption isotherms*

Adsorption isotherm for the sorption of  $\text{Hg}^{2+}$  ions was done at 25°C to check the efficiency of IIP. In present study Langmuir and Freundlich equation were tested.

$$\frac{1}{q_e} = \frac{1}{Q_m b C_e} + \frac{1}{Q_m}$$

where  $C_e$  ( $\text{mg L}^{-1}$ ) is the amount of total  $\text{Hg}^{2+}$  ions in the solution,  $q_e$  ( $\text{mg g}^{-1}$ ) is the  $\text{Hg}^{2+}$  ions adsorption capacity at equilibrium.  $Q_m$  the monolayer adsorbent capacity and  $b$  is the energy Langmuir constant of adsorption. The  $Q$  value was calculated from the slope of a linear plot of  $C_e/C_{\text{ads}}$  versus  $C_e$ . The correlated parameters were obtained by calculation from the values of the slope and intercept of the respective linear plot **Figure 9A**.

Freundlich is an empirical adsorption isotherm model which accounts for the multilayer adsorption by the adsorbent and favors the heterogeneous material. The linear Freundlich isotherm is given as:

$$\log C_{\text{ads}} = \log K_f + \frac{1}{n} \log C_e$$

where  $C_{\text{ads}}$  is the amount of mercury adsorbed per unit weight on the adsorbent ( $\text{mg g}^{-1}$ ), whereas  $C_e$  is concentration of mercury in solution ( $\text{mg L}^{-1}$ ) at equilibrium,  $K_f$  is the Freundlich capacity factor and 'n' is Freundlich intensity factor. Freundlich isotherm constants of the sorbent **Figure 9B**, were obtained from the slope and intercept calculation of the linear plot  $\log C_{\text{ads}}$  vs.  $\log C_e$ .

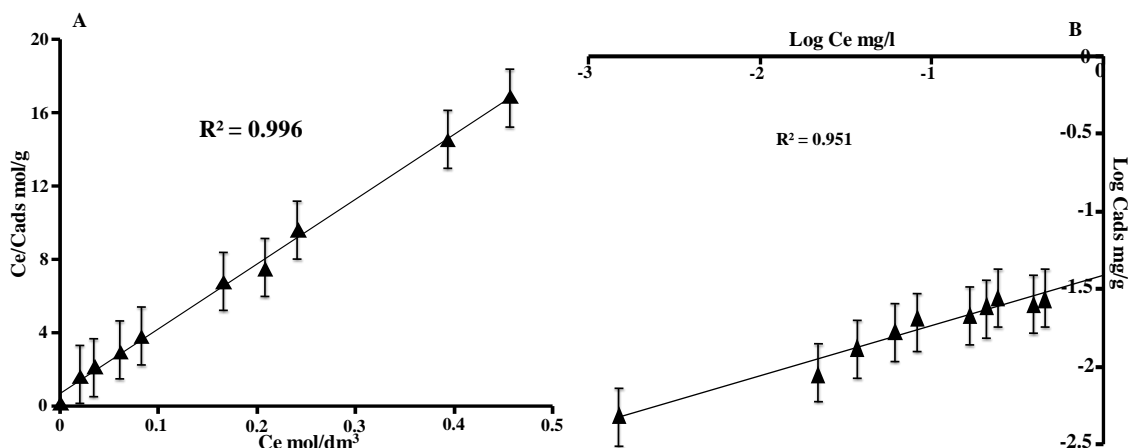


**Figure 9.** Langmuir adsorption isotherm (A) Freundlich adsorption isotherms (B)

**Table 1.** Mercury (II): Langmuir and Freundlich isotherm constants

Langmuir				Freundlich		
Q (mg/g <sup>-1</sup> )	L (L mg <sup>-1</sup> )	R <sub>L</sub>	R <sup>2</sup>	K <sub>f</sub> (mg/g <sup>-1</sup> )	n	R <sup>2</sup>
0.0282	51.96	0.018-0.161	0.996	0.346	3.11	0.951

The correlation coefficient ( $R^2$ ) of Langmuir and Freundlich were calculated and presented in **Table 1** along with other results and, from it can be concluded that adsorption of  $Hg^{2+}$  ions by IIP best adjust in Langmuir equation and it's a monolayer adsorption.

### Adsorption kinetics

In order to investigate the adsorption mechanism completely, adsorption equilibriums are needed to be equipped with adsorption kinetics [26] which helps in finding out the rate of metal ion adsorption and the time required to achieve equilibrium for mercury in aqueous environment. Pseudo first order and second order kinetic models were used to fit the experimental data. The pseudo first order rate constant  $K_1$  was determined from the plot in **Figure 10A** in which  $\log(q_e - q_t)$  versus  $t$  was plotted and a straight line was obtained for  $Hg^{2+}$  ion imprinted polymer and correlation factor value was ( $R^2=0.8907$ ). The experimental data was further analyzed for pseudo second order kinetic model by plotting  $t/q$  against  $t$  in **Figure 10B** and the second order rate constant was determined from the plot with correlation factor ( $R^2=0.9994$ ) and from above plots it can be concluded that pseudo second order kinetic model has good correlation for  $Hg^{2+}$  ions adsorption, and the Sorption kinetics constant obtained from the pseudo-first and second order models are given in **Table 2**. The Lagergren pseudo 1st order and pseudo 2nd order linearized models are given by equations (4) and (5).

$$\log(q_e - q_t) = \log q_e - k_{1ads} \frac{t}{2.303} \quad (4)$$

$$\frac{t}{q_1} = \frac{1}{k_2 q_e} + \frac{t}{q_1} \quad (5)$$

where:

- $K_{1,ads}$  is Lagergren rate constant for first order sorption ( $\text{min}^{-1}$ )
- $K_2$  is second order rate constant ( $\text{g ug}^{-1} \text{min}^{-1}$ )
- $q_t$  is amount of adsorbate adsorbed at time  $t$
- $q_e$  is amount of adsorbate adsorbed at equilibrium.

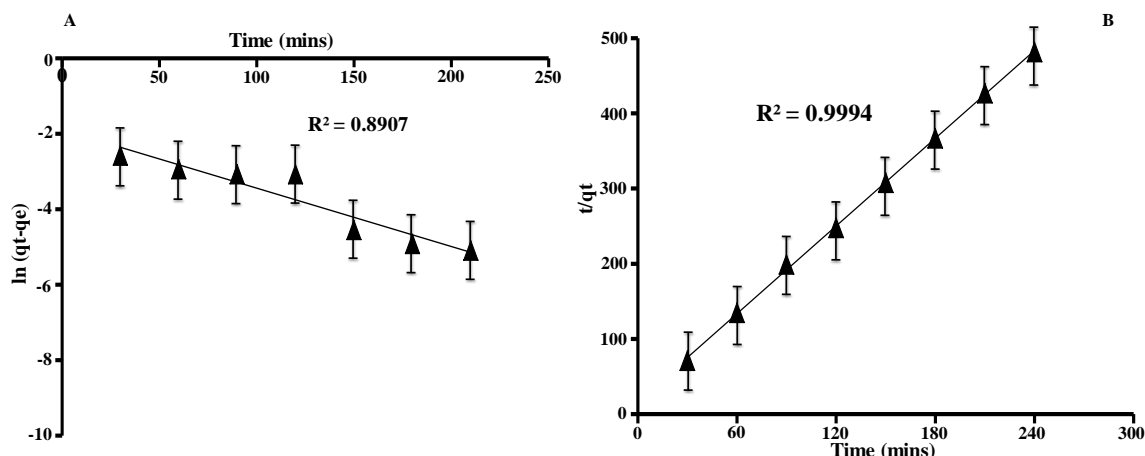


Figure 10. Pseudo 1st order kinetics (A) Pseudo 2nd order kinetics (B)

Table 2. Kinetic model parameters for the sorption of  $Hg^{2+}$  ions by IIP

Pseudo first order			Pseudo second order		
$K_1$ ( $min^{-1}$ )	$q_e$ , cal ( $mg\ g^{-1}$ )	$R^2$	$K_2$ ( $min^{-1}$ )	$q_e$ , cal ( $mg\ g^{-1}$ )	$R^2$
0.029	0.47	0.887	0.221	0.51	0.999

Table 3.  $K_d$ ,  $K$  and  $k'$  values for  $Cu^{2+}$ ,  $Cr^{3+}$ , and  $Co^{2+}$  with respect to  $Hg^{2+}$

Metal ion	Non-imprinted polymer		Imprinted polymer		
	$K_d$	$k$	$K_d$	$k$	$k'$
$Hg^{2+}$	1.92		10.27		
$Cu^{2+}$	0.123	15.60	0.084	122	7.82
$Cr^{3+}$	0.137	14.01	0.099	103	7.35
$Co^{2+}$	0.311	6.17	0.013	76	12.31

### Selectivity Study

The distribution and selectivity coefficient of competitive ions can be obtained by equilibrium data according to equation 1, 2 and 3. In equation 1  $K_d$  is distribution coefficient,  $C_i$  and  $C_f$  are initial and final concentrations of metal ions.  $V$  is the volume of the solution in (mL) while  $m$  is the mass of adsorbent used in (g).  $k$  is the selectivity coefficient,  $X^{m+}$  represents competitive ions.

$$k_d = \left[ \frac{(c_i - c_f)}{c_f} \right] (v/m) \quad (1)$$

$$k = K_d(M^+)/K_d(X^{m+}) \quad (2)$$

A comparison of  $k$  values of imprinted polymer with non-imprinted polymer was given by relative selectivity coefficient  $k'$

$$k' = k_{imprinted}/k_{non-imprinted} \quad (3)$$

Competitive adsorption of  $Hg^{2+}$  ions and other interfering ions which contain the same charge, nearly identical size and have good binding affinity with carboxylic group were also investigated via batch experiment.  $Cu^{2+}$ ,  $Cr^{3+}$ , and  $Co^{2+}$  were chosen because they possess same atomic radii. Comparison of the  $K_d$  values for the IIP samples with NIP shows an increase in  $K_d$  for  $Hg^{2+}$  while  $K_d$  decrease for  $Cu^{2+}$ ,  $Cr^{3+}$ , and  $Co^{2+}$ . The relative selectivity coefficient signifies the metal adsorption affinity of recognition sites for  $Hg^{2+}$  ions. Table 3 shows that relative selectivity coefficient of imprinted polymer for  $Hg^{2+} / Cu^{2+}$ ,  $Hg^{2+} / Cr^{3+}$ ,  $Hg^{2+} / Co^{2+}$  were respectively 122, 103, 76 times greater than for non-imprinted polymer.

### Analytical Application

Initially all procedures were performed in aqueous medium while optimization of parameters and later on, IIP was applied for decontamination of drinking water which were collected from diverse water sources available for drinking purpose in the region and, IIP showed efficient adsorption capacity for  $Hg^{2+}$  ions. Results show high amount of mercury contamination, it could be due to effluent discharged from industries without any treatment.

**Table 4.** Standard Addition to water sample method for Hg<sup>2+</sup> n=5 (µg L<sup>-1</sup> ± Error)

Sample	S1	S2	S3	S4	S5
Without addition	15.3±0.6	12.1±0.5	14.3±0.71	16.5±0.51	18.23±0.62
Hg <sup>2+</sup> Added	5	5	5	5	5
Hg <sup>2+</sup> Found	20.1±0.7	17.0±0.61	19.0±0.55	21.3±0.39	23.1±0.45
% recovery	96	98	94	96	97.4

Amount of mercury in all water samples were beyond permissible limit of WHO drinking water standards. The detoxification process of water samples was carried out at optimum conditions. The results are given in **Table 4**, which presents that mercury level in each sample decreased below acceptable limits.

## CONCLUSION

In this paper an adsorbent Hg<sup>2+</sup> ions imprinted polymer was synthesized via precipitation method in which bi functional reagent 1-vinylimidazole was used as a monomer and metal-complexing group and characterized successfully by FTIR, SEM and EDX. IIP showed higher selectivity for Hg<sup>2+</sup> ions then other interfering ions Cu<sup>2+</sup>, Cr<sup>3+</sup>, and Co<sup>2+</sup> based on selectivity study. Adsorption favors the second order kinetics and follows the Langmuir's isotherm. Fast and easy method for the synthesis of Hg<sup>2+</sup> ions imprinted polymer is reported in this work. Focus of research work was detoxification of Hg<sup>2+</sup> ions and IIP's are best alternative for removal of toxins from aqueous medium then earlier reported method.

## REFERENCES

- Trasande L, Landrigan PJ, Schechter C. Public health and economic consequences of methyl mercury toxicity to the developing brain. *Environmental health perspectives*. 2005;590-596. <https://doi.org/10.1289/ehp.7743>
- Manahan SM. *Environmental Chemistry* Lewis Publishers Michigan. 1994.
- Ganjali MR, Alizadeh T, Azimi F, Larjani B, Faridbod F, Norouzi P. Bio-mimetic ion imprinted polymer based potentiometric mercury sensor composed of nano-materials. *Int. J. Electrochem. Sci.* 2011;6(11):5200-8.
- Böse-O'Reilly S, Drasch G, Beinhoff C, Maydl S, Vosko MR, Roeder G, Dzaja D. The Mt. Diwata study on the Philippines 2000 – Treatment of mercury intoxicated inhabitants of a gold mining area with DMPS (2, 3-Dimercapto-1-propane-sulfonic acid, Dimaval®). *Science of the Total Environment*. 2003;307(1):71-82. [https://doi.org/10.1016/S0048-9697\(02\)00547-8](https://doi.org/10.1016/S0048-9697(02)00547-8)
- Alizadeh T, Ganjali MR, Zare M. Application of an Hg<sup>2+</sup> selective imprinted polymer as a new modifying agent for the preparation of a novel highly selective and sensitive electrochemical sensor for the determination of ultratrace mercury ions. *Analytica chimica acta*. 2011;689(1):52-9. <https://doi.org/10.1016/j.aca.2011.01.036>
- Crinnion WJ. Maternal levels of xenobiotics that affect fetal development and childhood health. *Alternative medicine review*. 2009;14(3):212-23.
- van Genuchten CM, Addy SE, Peña J, Gadgil AJ. Removing arsenic from synthetic groundwater with iron electrocoagulation: an Fe and As K-edge EXAFS study. *Environmental science & technology*. 2012;46(2):986-94. <https://doi.org/10.1021/es201913a>
- Levy IK, Mizrahi M, Ruano G, Zampieri G, Requejo FG, Litter MI. TiO<sub>2</sub>-photocatalytic reduction of pentavalent and trivalent arsenic: production of elemental arsenic and arsine. *Environmental science & technology*. 2012;46(4):2299-308. <https://doi.org/10.1021/es202638c>
- Rao TP, Daniel S, Gladis JM. Tailored materials for preconcentration or separation of metals by ion-imprinted polymers for solid-phase extraction (IIP-SPE). *TrAC Trends in Analytical Chemistry*, 23(1), 28-35. K.K. Sirkar, *Ind. Chem. Res.* 2004;47(2008):5250-66.
- Rubio J, Souza ML, Smith RW. Overview of flotation as a wastewater treatment technique. *Minerals engineering*. 2002;15(3):139-55. [https://doi.org/10.1016/S0892-6875\(01\)00216-3](https://doi.org/10.1016/S0892-6875(01)00216-3)
- Chen G. Electrochemical technologies in wastewater treatment. *Separation and purification Technology*. 2004;38(1):11-41. <https://doi.org/10.1016/j.seppur.2003.10.006>
- Srivastava NK, Majumder CB. Novel biofiltration methods for the treatment of heavy metals from industrial wastewater. *Journal of hazardous materials*. 2008;151(1):1-8. <https://doi.org/10.1016/j.jhazmat.2007.09.101>
- Addo Ntim S, Mitra S. Adsorption of arsenic on multiwall carbon nanotube-zirconia nanohybrid for potential drinking water purification. *Journal of Colloid and Interface Science*. 2012;375(1):154-9. <https://doi.org/10.1016/j.jcis.2012.01.063>

14. Wulff G. Molecular imprinting in cross-linked materials with the aid of molecular templates—a way towards artificial antibodies. *Angewandte Chemie International Edition in English*. 1995;34(17):1812-32. <https://doi.org/10.1002/anie.199518121>
15. Mosbach K, Haupt K. Some new developments and challenges in non-covalent molecular imprinting technology. *Journal of molecular recognition*. 1998;11(1-6):62-8. [https://doi.org/10.1002/\(SICI\)1099-1352\(199812\)11:1/6<62::AID-JMR391>3.0.CO;2-5](https://doi.org/10.1002/(SICI)1099-1352(199812)11:1/6<62::AID-JMR391>3.0.CO;2-5)
16. Albericio F, Tulla-Puche J. (Eds.). *The power of functional resins in organic synthesis*. John Wiley & Sons. 2008.
17. Sharma AK, Lee BK. Lead sorption onto acrylamide modified titanium nanocomposite from aqueous media. *Journal of environmental management*. 2013;128:787-97. <https://doi.org/10.1016/j.jenvman.2013.06.030>
18. Yan D, Yang L, Wang Q. Alternative thermodiffusion interface for simultaneous speciation of organic and inorganic lead and mercury species by capillary GC-ICPMS using tri-n-propyl-lead chloride as an internal standard. *Analytical chemistry*. 2008;80(15):6104-9. <https://doi.org/10.1021/ac800347j>
19. Daniel S, Rao PP, Rao TP. Investigation of different polymerization methods on the analytical performance of palladium (II) ion imprinted polymer materials. *Analytica chimica acta*. 2005;536(1):197-206. <https://doi.org/10.1016/j.aca.2004.12.052>
20. Amin F, Talpur FN, Balouch A, Chandio ZA, Surhio MA, Afridi HI. Biosorption of mercury (II) from aqueous solution by fungal biomass *Pleurotus eryngii*: Isotherm, kinetic, and thermodynamic studies. *Environmental Progress & Sustainable Energy*. 2016;35(5):1274-82. <https://doi.org/10.1002/ep.12342>
21. Bleiman N, Mishael YG. Selenium removal from drinking water by adsorption to chitosan-clay composites and oxides: batch and column tests. *Journal of Hazardous Materials*. 2010;183(1):590-5. <https://doi.org/10.1016/j.jhazmat.2010.07.065>
22. Fosso-Kankeu E, Mulaba-Bafubiandi AF, Mamba BB, Barnard TG. Prediction of metal-adsorption behaviour in the remediation of water contamination using indigenous microorganisms. *Journal of environmental management*. 2011;92(10):2786-93. <https://doi.org/10.1016/j.jenvman.2011.06.025>
23. Liu Y, Sun X, Li B. Adsorption of Hg 2+ and Cd 2+ by ethylenediamine modified peanut shells. *Carbohydrate Polymers*. 2010;81(2):335-9. <https://doi.org/10.1016/j.carbpol.2010.02.020>
24. Mason RP, Fitzgerald WF, Morel FM. The biogeochemical cycling of elemental mercury: anthropogenic influences. *Geochimica et Cosmochimica Acta*, 1994;58(15):3191-3198.
25. Khajeh M, Yamini Y, Ghasemi E, Fasihi J, Shamsipur M. Imprinted polymer particles for selenium uptake: synthesis, characterization and analytical applications. *Analytica chimica acta*. 2007;581(2):208-213.
26. Amin F, Talpur FN, Balouch A, Surhio MA, Bhutto MA. Biosorption of fluoride from aqueous solution by white-rot fungus *Pleurotus eryngii* ATCC 90888. *Environmental Nanotechnology, Monitoring & Management*. 2015;3:30-37.

<http://www.eurasianjournals.com>